Supporting Information for "Snow Loss into Leads in Arctic Sea Ice: Minimal in Typical Wintertime Conditions, but High During a Warm and Windy Snowfall Event"

David Clemens-Sewall[1], Chris Polashenski[1,2], Markus M. Frey[3], Christopher J. Cox[4], Mats A. Granskog[5], Amy R. Macfarlane[6], Steven W. Fons[7,8], Julia Schmale[9], Jennifer K. Hutchings[10], Luisa von Albedyll[11], Stefanie Arndt[11], Martin Schneebeli[6], Don Perovich[1]

[1]Thayer School of Engineering, Dartmouth College, Hanover, NH, USA

[2]Cold Regions Research and Engineering Laboratory, US Army Corps of Engineers, Hanover, NH, USA

[3]British Antarctic Survey – Natural Environment Research Council, Cambridge, UK

[4]NOAA Physical Sciences Laboratory, Boulder, CO, USA

[5]Norwegian Polar Institute, Fram Centre, Tromsø, Norway

[6]WSL Institute for Snow and Avalanche Research SLF, Davos, Switzerland

[7]Cryospheric Sciences Laboratory, NASA Goddard Space Flight Center, Greenbelt, MD, USA

[8]Earth System Science Interdisciplinary Center, University of Maryland, College Park, MD, USA

[9]Extreme Environments Research Laboratory, École Polytechnique Fédérale de Lausanne, Sion, Switzerland

[10]College of Earth, Ocean, and Atmospheric Sciences, Oregon State University, Corvallis, OR, USA

[11]Alfred-Wegener-Institut, Helmholtz-Zentrum für Polar- und Meeresforschung, Bremerhaven, Germany

January 8, 2023, 4:22pm

Contents of this file

1. Text S1 and S2
2. Figures S1 and S2
3. Tables S1 and S2

Introduction

The supporting information presented here includes ancillary details about the leads sampled (Section S1 and Figure S1) and the isotopic composition of snow-free ice and snow (Section S2, Figure S2, and Tables S1&S2). This information is also available with the published data set (Clemens-Sewall et al., 2022).

S1. Lead Descriptions

S1.1 SL Lead

The SL lead (named for 'Stern Lead') extended more than 1 km aft and starboard of Polarstern (Figure S1). On 15 April at approximately 84.32°N, 13.77°E, we collected 12 ice cores from two transects (sample spacing 2.5 m) in the SL lead approximately 100 m from the stern of Polarstern. At this location, the lead was approximately 40 m wide. In the upwind half(relative to the winds 25 and 29 March), there were two 10-m-wide, flat pans of ice. The pans were separated by separated by a 50 cm tall ridge. The downwind half was a mixture of ridges and rubble. All samples came from the two flat pans on the upwind half. One transect was perpendicular to the lead and extended 20 m from the upwind edge across both pans (we did not core the small ridge). The other transect ran for 12 m parallel to the lead and was approximately 5 m from the upwind edge of the lead.

The transects intersected in the middle of the upwind pan, and the ice core at this site (DC_SL_5) was vertically sectioned. All other cores were collected as bulk samples. Some cores were underlain by a gap layer of water and then additional rafted blocks of ice. In general we collected ice just down to the gap layer, however for one core (DC_SL_2) some of the ice below the gap was accidentally collected.

S1.2 M Lead

The M lead, named for the nearby Met City ('MET' on Figure S1 Shupe et al., 2022) separated Met City from the Leg 2 Remote Sensing site (see Nicolaus et al., 2022). We collected 8 cores across the entire width of M lead with a spacing of 1 m on 18 April at approximately 84.48°N, 13.95°E. We sectioned a core from the center of the transect (DC_M_5) and the core closest to the Met City side (DC_M_1). All other cores were collected as bulk samples.

S1.3 T Lead

The T lead (named for the 'Southern' snow and ice thickness Transect) opened on 4 April across the Snow1 sampling area, the S Transect, and adjacent to the Stakes3 mass balance site (Figure S1; Nicolaus et al., 2022). During 5–8 April, ice dynamics occurred in the center of the T lead but not where we would subsequently collect samples from. On 15 April at approximately 84.32°N, 13.77°E, we collected 14 ice cores from two transects in the downwind half of the T lead. The T lead was approximately 20 m wide and was split in the middle by a crack running parallel to the lead that opened the morning we sampled. One transect was perpendicular to the lead and extended 10 m from the downwind edge to the crack (sample spacing 1 m). The other transect ran for 10 m parallel to the lead and

was approximately 5 m from the downwind edge. The transects intersected in the middle, and the ice core at this site (DC_T_17) was sectioned. All other cores were collected as bulk samples. Unfortunately, we were unable to access the ice on the upwind half of the lead on 15 April and this ice ridged in the following days.

S1.4 A Lead

The A lead opened on 19 April along the edge of the Snow2 sampling area (Figure S1; Nicolaus et al., 2022) during a warm air intrusion that caused. Most of the leads from 19–20 April ridged and rafted on 21–22 April. However a 6x100 m section of A lead that we would subsequently sample was protected from the ice dynamics by two second-year-ice floes. On 24 April at approximately 84.03°N, 15.87°E, we collected 6 ice cores in a transect across A lead with 1 m spacing. We sectioned a core in the middle (DC_A_3) and all other cores were collected as bulk samples. The core on the side closest to Polarstern (DC_A_6) was noticeably softer than the other cores (i.e. a snow ruler easily went through to the ocean). For all cores, there was not a clear distinction between snow and ice. Although the uppermost 5 cm were softer than below, it appeared that the entire core was composed of the same material. When we revisited A lead on 28 April at approximately 84.03°N, 16.65°E, we collected and sectioned a single core (DC_A_7) from the center of A lead one meter away from DC_A_3.

S2. δ^{18}O of Snow-Free Ice and Snow

Two lines of evidence suggest that most or all of the blowing snow available to be deposited in leads during the A Lead event was from concurrent or very recent precipitation. First, on 16 April (three days prior to the A Lead event) air temperatures warmed up to

near freezing, which created patchy glaze crusts and a sintered, hard-to-erode snow surface. Second, as mentioned in the main text, there were three stations that observed the snow surface height with sonic rangers (1 min avg of 1 Hz sampling) positioned over level ice within 1 km of Polarstern—near Met City ('MET' on Figure S1), Balloon Town ('BT' on Figure S1), and BGC1 (Figure S1). These stations did not observe any erosion of the snow that pre-dated 19 April, but they observed 100% erosion of snow that was deposited during 19–21 April. This indicates that it was new snow, not eroded old snow, that was blowing during the event. We identified two surface snow samples that were deposited during the A lead event. One came from a snow drift on 'David's Ridge' (Figure S1) and the other was a snow pit near the Remote Sensing site ('RS' on Figure S1). The δ^{18}O of these snow samples was very similar, -14.4 ‰and -14.2 ‰respectively.

As mentioned in the main text, we use the δ^{18}O measurements from bottom ice samples from the sectioned cores to determine the isotopic composition of snow-free ice (Granskog et al., 2017). Unfortunately, a number of the subsamples were damaged during transit and had to be excluded. Thus we have fewer bottom ice samples (Table S1) than intended, especially for the SL lead (only one sample was usable out of the five that we collected). The δ^{18}O of each usable bottom ice sample was within the measurement uncertainty of all other samples (Figure S2b; note that the error bars are all overlapping). Given this overlap, and that the ice was formed from the same seawater at approximately the same temperature, it is likely that the isotopic composition of snow-free ice for the SL, M, and T leads is essentially the same and most of the variation in mean values (Table S1) is due to measurement noise. For this reason, we combined all bottom ice samples to estimate

the distribution of δ_{ref} used for all leads in the main text (the line labelled 'All' in Table S1). To investigate the sensitivity of our results to this choice, we repeated the analysis of snow loss into each lead with δ_{ref} estimated from just the bottom ice samples of that lead (Table S2). The only notable difference is that for the SL lead using δ_{ref} from its bottom ice sample yields a mean snow loss of 1.2 cm instead of 2.2 cm SWE. Note that if this were the case it would actually reinforce the key finding that little snow is lost under typical wintertime conditions. For the A lead, the entire cores were granular, thus there are no bottom ice samples. In the main text we use the same δ_{ref} as the other leads. To test the sensitivity of this assumption, we repeated the analysis for the A lead with δ_{ref} prescribed to be 0.0 ‰(as has been previously assumed: e.g., Jeffries et al., 1997). This assumption would slightly reduce the snow loss into the A lead (Table S2), but does not change the key findings of this work.

References

Clemens-Sewall, D., Macfarlane, A., Fons, S., Granskog, M., Hutchings, J., & Schmale, J. (2022). Salinity and Stable Water Isotopes for Ice Cores in Leads during Leg 3 of the Multidisciplinary drifting Observatory for the Study of Arctic Climate 2020. *Arctic Data Center*. Retrieved 2023-01-08, from `https://arcticdata.io/catalog/view/doi%3A10.18739%2FA23N20G15` (Publisher: Arctic Data Center) doi: 10.18739/A23N20G15

Granskog, M. A., Rösel, A., Dodd, P. A., Divine, D., Gerland, S., Martma, T., & Leng, M. J. (2017, March). Snow contribution to first-year and second-year Arctic sea ice mass balance north of Svalbard. *Journal of Geophysical Research: Oceans*, 2539–

2549. Retrieved 2018-09-26, from https://agupubs.onlinelibrary.wiley.com/doi/abs/10.1002/2016JC012398%4010.1002/%28ISSN%292169-9291.NICE1 doi: 10.1002/2016JC012398@10.1002/(ISSN)2169-9291.NICE1

Hutter, N., Hendricks, S., Jutila, A., Ricker, R., von Albedyll, L., Birnbaum, G., & Haas, C. (2021, July). *Gridded airborne laserscanner (ALS) elevation data (L4) for three flights during MOSAiC (prerelease).* Zenodo. Retrieved 2022-08-19, from https://zenodo.org/record/5121823 (Version Number: 1.0.0-alpha Type: dataset) doi: 10.5281/ZENODO.5121823

Jeffries, M. O., Morris, K., Weeks, W. F., & Worby, A. P. (1997). Seasonal variations in the properties and structural composition of sea ice and snow cover in the Bellingshausen and Amundsen Seas, Antarctica. *Journal of Glaciology*, *43*(143), 138–151. Retrieved 2022-06-19, from https://www.cambridge.org/core/journals/journal-of-glaciology/article/seasonal-variations-in-the-properties-and-structural-composition-of-sea-ice-and-snow-cover-in-the-bellingshausen-and-amundsen-seas-antarctica/D4475C2D538E87C677BB94FCDA38AF06 (Publisher: Cambridge University Press) doi: 10.3189/S0022143000002902

Nicolaus, M., Perovich, D. K., Spreen, G., Granskog, M. A., von Albedyll, L., Angelopoulos, M., ... Wendisch, M. (2022, February). Overview of the MOSAiC expedition: Snow and sea ice. *Elementa: Science of the Anthropocene*, *10*(1), 000046. Retrieved 2022-02-07, from https://doi.org/10.1525/elementa.2021.000046 doi: 10.1525/elementa.2021.000046

Shupe, M. D., Rex, M., Blomquist, B., Persson, P. O. G., Schmale, J., Uttal, T., ... Yue, F. (2022, February). Overview of the MOSAiC expedition: Atmosphere. *Elementa: Science of the Anthropocene*, *10*(1), 00060. Retrieved 2022-06-19, from https://doi.org/10.1525/elementa.2021.00060 doi: 10.1525/elementa.2021.00060

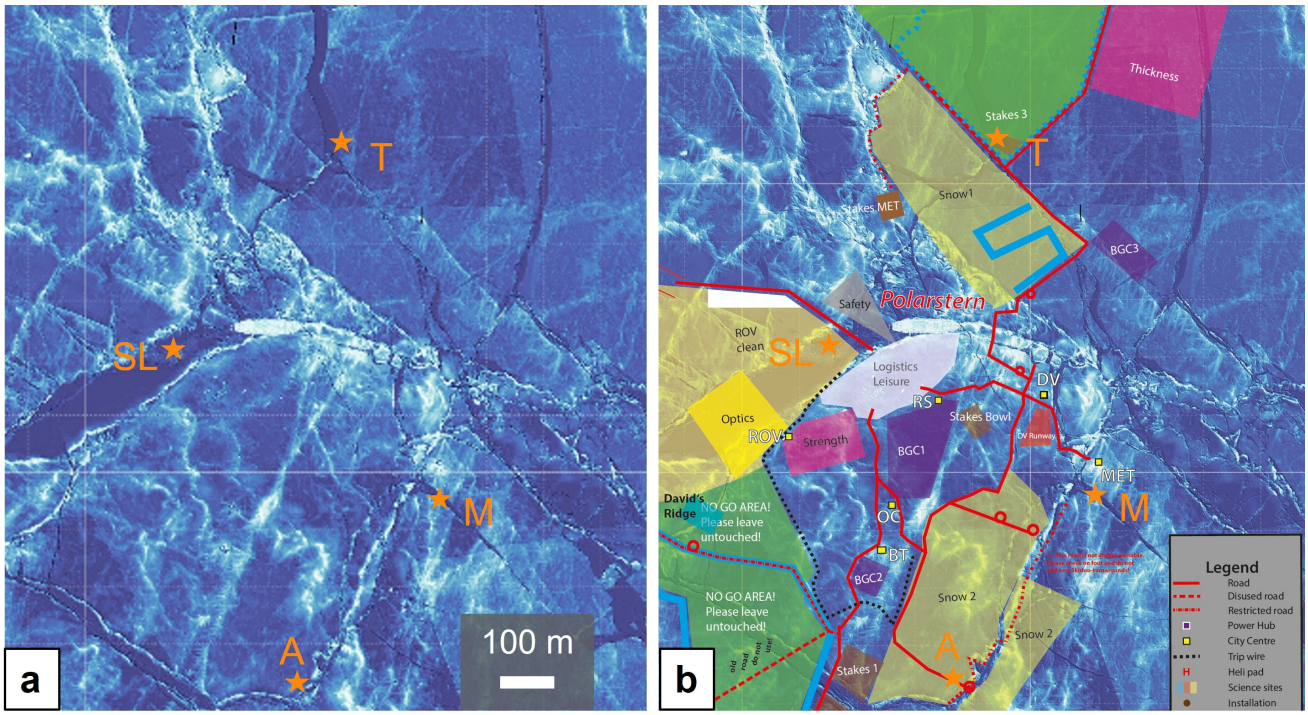

Figure S1. Map of the MOSAiC field site with lead locations indicated by orange stars and labels. The underlying topographic basemap is derived from Airborne Laser Scanning data collected on 8 April 2020 (Hutter et al., 2021). The basemap has been hillshaded such that high areas (e.g., pressure ridges, Polarstern) are white and lower areas are blue. Lead locations are shown on just the topography (a) and on an operational map of the roads and research sites used during the expedition (b). Note that the topography data was collected before the A lead formed. Hence it is not present in the basemap. Thank you to Robert Ricker and Manuel Ernst for processing these data and creating maps respectively while onboard.

Table S1. Parameters for δ_{ref}

Lead	# Bottom ice samples	μ_{ref} (‰)	τ_{ref} (‰)
All	11	2.24	0.15
SL	1	1.81	0.50
M	7	2.17	0.19
T	3	2.54	0.29

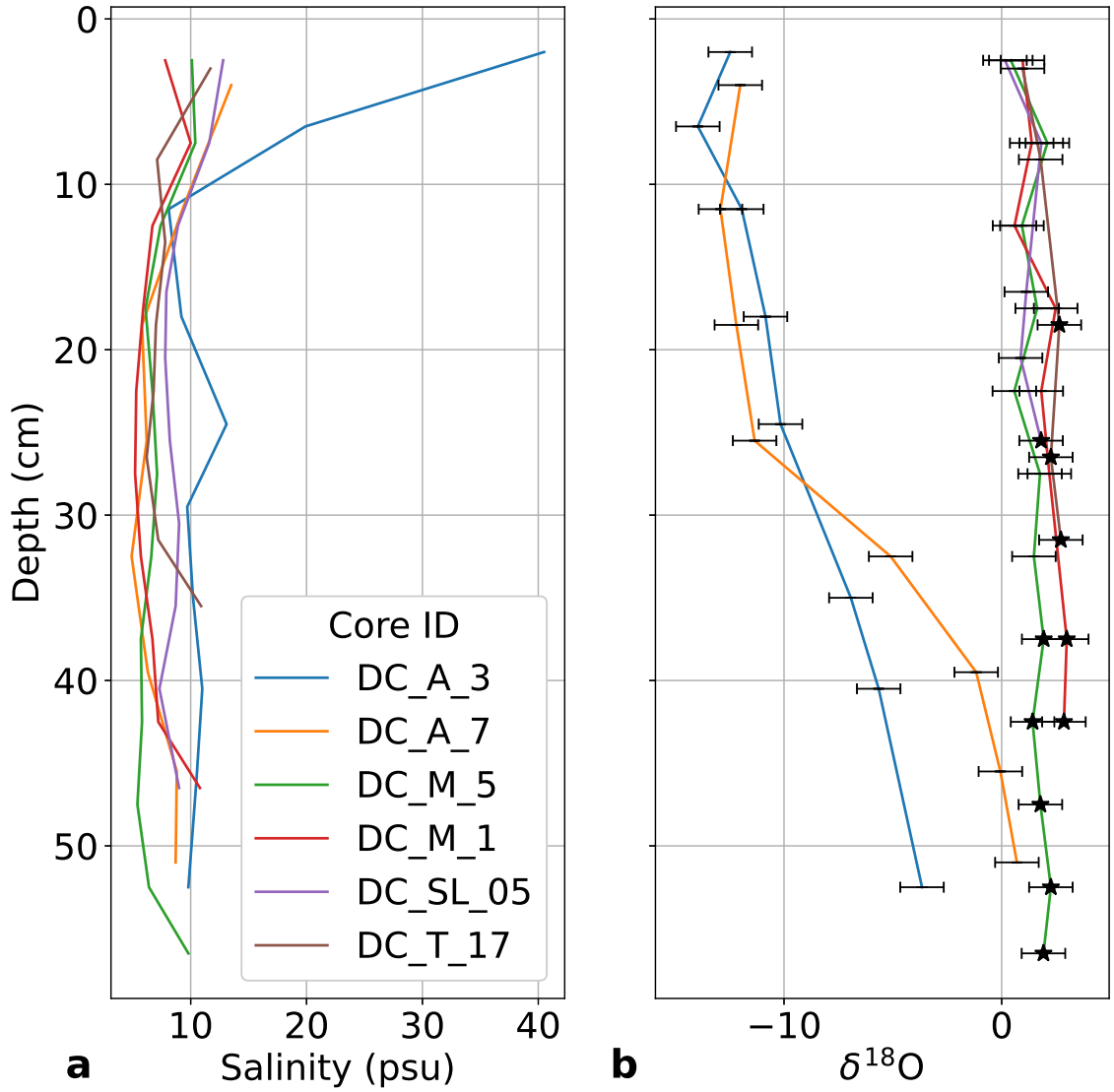

Figure S2. Salinity (a) and δ^{18}O (b) profiles for the sectioned cores. The 'Core ID' for each core includes the lead which it came from (e.g., 'DC_A_3' was the third core in the A lead). The measurement uncertainty at the 95% confidence level in displayed in the horizontal error bars in (b). In (b) samples classified as 'bottom ice' (below the lowermost granular layer) are marked with black stars. Note, if the δ^{18}O subsample was damaged and unusable, we do not display it in (b). This means that in some profiles at some depths, we have salinity data (a) but not δ^{18}O data.

Table S2. Snow Loss with Different Assumptions for δ_{ref}

Lead	δ_{ref} Source	Mean SWE (cm)	95% credible interval (cm)
SL	All	2.2	[1.5, 3.0]
	SL	1.2	[0.4, 2.0]
M	All	0.6	[0.1, 1.2]
	M	0.5	[0.0, 1.1]
T	All	0.1	[0.0, 0.4]
	T	0.3	[0.0, 0.7]
A	All	35.0	[33.9, 36.1]
	0[a]	32.4	[31.2, 33.6]

[a] As described in Section S2, this line is if we assume that $\delta_{ref} = 0$ ‰for the A lead.